

## 5.1: Electric Field Analysis in TFT-LCDs with In-Plane Switching Mode of Nematic LCs

*M. Ohta, M. Yoneya\*, K. Kondo\**

Electron Tube & Devices Division, Hitachi, Ltd., Chiba, Japan

\*Hitachi Research Laboratory, Hitachi, Ltd., Ibaraki, Japan

### Abstract

Influences of unfavorable electric fields were analyzed, to identify means for suppressing crosstalk in TFT-LCDs with an in-plane switching (IPS) mode. An optimum electrode configuration and size parameters which effectively shield these fields was obtained and a 13.3 inch diagonal crosstalk-free IPS TFT-LCD was developed.

### Introduction

Recently, LCD monitors are beginning to replace CRT monitors for desktop PCs and workstations because of their lower power consumption and better space saving property in comparison with CRTs. The in-plane switching (IPS) mode proposed by the Baur group[1-4] is suitable for LCD monitors owing to their extremely wide viewing-angle characteristics comparable to those of CRTs[1-8]. We introduced use of TFT arrays to get the best properties from the IPS mode and we developed the first prototype of a 10.4 inch diagonal IPS TFT-LCD with VGA resolution[9,10]. However, there are several problems when combining the IPS mode with TFT arrays. The most serious problem is unfavorable electric fields (noise) from other electrodes (or bus-lines) of the TFT arrays to pixel areas. With IPS TFT-LCDs, their optical properties are easily degraded by noise because liquid crystal (LC) molecules are not surrounded by driving electrodes as in conventional TN TFT-LCD. In particular, the influences of the electric potential of the source bus-lines on that of the pixel electrodes and the electric field between the pixel electrodes and the counter electrodes are significant since the potential of the source bus-line continuously varies as the imaging signal is propagated to the pixel electrodes through the TFTs in each array row. Therefore, suppression of these influences is a key point for combining the TFTs with the IPS mode.

In this paper, we analyze the influences of the noise on the TFT arrays as a function of their electrode configuration. In particular, we consider which electrode configuration is the most suitable for pixels of the IPS-TFT-LCDs with regard to suppressing the noise and which size parameters of the electrodes and bus-lines are the best. Based on the optimized configuration of the electrodes and bus-lines, we designed a 13.3 inch diagonal IPS TFT-LCD for monitor use which has crosstalk-free.

### Crosstalk on IPS-TFT-LCDs

First, we describe the mechanisms of crosstalk generation on the IPS TFT-LCDs. Crosstalk caused by the source bus-line potential has two origins. One is capacitive coupling between the source bus-lines and the pixel electrodes, as in a conventional TN TFT-LCD. Since the potential of the pixel electrode is a floating potential determined by constant charge, fluctuation of the pixel electrode potential  $\Delta V_p$  is expressed by the following equation.

$$\Delta V_p = (C_{sp}/C_T) \Delta V_s \cdots (1)$$

Here,  $\Delta V_s$ ,  $C_{sp}$  and  $C_T$  represent variations of the source bus-line potential, capacitance between the source bus-line and a pixel electrode, and total capacitance of a pixel, respectively. Compared to the TN TFT-LCD,  $C_T$  is very small because the electrodes are arranged on the same substrate plane. Therefore, in order to suppress  $\Delta V_p$  on the IPS TFT-LCD,  $C_{sp}$  has to be smaller than that of the TN TFT-LCD.

The second origin is the leakage of the source bus-line potential to the optical switching medium in a pixel between the two electrodes which are driving the LCs. This is peculiar to the IPS TFT-LCD since in the TN TFT-LCD the optical switching medium is sandwiched between the two planar electrodes. For this type of crosstalk, the dielectric and resistance properties of the materials such as LCs, alignment films, passivation layers, color filters and the black matrix(BM), and the electrode configuration are significant parameters. The material parameters are not controllable, while the electrode configuration can be controlled through the pixel design. Therefore, optimization of the electrode configuration is necessary for shielding.

### Electrode configuration

Figures 1 and 2 show cross-sectional views of the conventional TN TFT-LCD and four types of structures for the IPS TFT-LCD, respectively.

The first structure of figure 2(a) is the simplest IPS TFT-LCD structure which analogous to the conventional TN-TFT-LCD of figure 1. The non-shielded structure has a pixel electrode located next to the source bus-line, thus there is no shielding effect from the source bus-line potential. Since most of the electric force lines from the source bus-line terminate in the adjacent pixel electrode for this configuration, the capacitance between the source bus-line and the pixel electrode  $C_{sp}$  in equation (1) is very large. Accordingly, the fluctuation of the pixel electrode potential given by equation (1) is caused by strong capacitive coupling between the source bus-line

and the pixel electrode, and serious crosstalk occurs.

Figures 2(b)-(d) show three structure having shielding effects. The completely shielded structure (figure 2(b)), in which the shielding electrode is located just above the source bus-line on the LC layers side, has the best shielding property because all of the electric force lines from the source bus-line are eliminated in the shielding electrode. However, this leads to high capacitive loads of the source bus-line and an impractical capability for the signal drivers is needed. Therefore, ordinary signal drivers which have a low current capability cannot be used. Furthermore, an additional fabrication process for the TFT arrays to make the shielding electrode on the top reduces the productivity.

For the BM shielded structure (figure 2(c)), a conductive BM, which has both a light shielding property and a conductivity performing perfectly as the shield electrode, is set on the counter substrate and a shielding potential is applied to the conductive BM. In this configuration, since the electric force lines terminate in the BM, the source bus-line potential is effectively shielded. Moreover, ordinary signal drivers can be used in this configuration because of low capacitive loads of the source bus-line, comparable to those of the TN-TFT-LCD. The conductive BM with a low reflectance properties such as CrO/Cr, is suited to this configuration; most metallic conductive BMs are

unsuitable because of their higher reflectance compared to those of a non-conductive resinous BM. Moreover, this configuration is complicated because the shielding potential has to be applied to the BM.

For the common shielded structure (figure 2(d)), a common electrode is located next to the source bus-line. The capacitive coupling between the source bus-line and the pixel electrode is smaller than in the non-shielded structure. Since most of the electric force lines also terminate in the adjacent common electrode, total crosstalk intensity can be reduced by the shielding effect of the common electrode potential which is constantly applied from the electric source.

Accordingly, we selected the common shielded structure and we used it in the prototype 10.4in./VGA IPS TFT-LCD reported in Asia Display '95. The structure is simplest and has low capacitive loads and low reflectance. However, the influences of the noise strongly depend on size parameter of the electrodes, especially their width. Therefore, we have to optimize the shielding effect of the common potential based on an investigation using 2-D device simulations of the IPS mode, similar to those of Dickmann et al.[11,12].

## Results

Figures 3 and 4 show simulation results for the case of a narrow common electrode, which has as its ratio of width of the common electrode ( $W_C$ ) to that of the source bus-line ( $W_S$ ) of  $W_C/W_S = 0.6$ , and the case of a wide common electrode, which has  $W_C/W_S = 1.5$ , respectively. Here, (a), (b) and (c) show distributions of electric potentials in the LC layer, in-plane rotation angles and tilt angles of LC molecule directors, respectively, where the source potential  $V_S = +5$ , the pixel potential  $V_P = -2.5$  V and the common potential  $V_C = 0$  V. We note that, for the wide common electrode, since the source potential has a greater attenuation normal to the substrate plane, the LC directors near the pixel

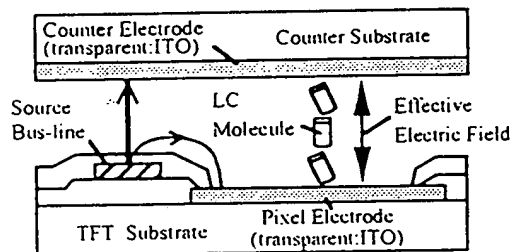


Figure 1. Cross sectional view of conventional TN TFT-LCD

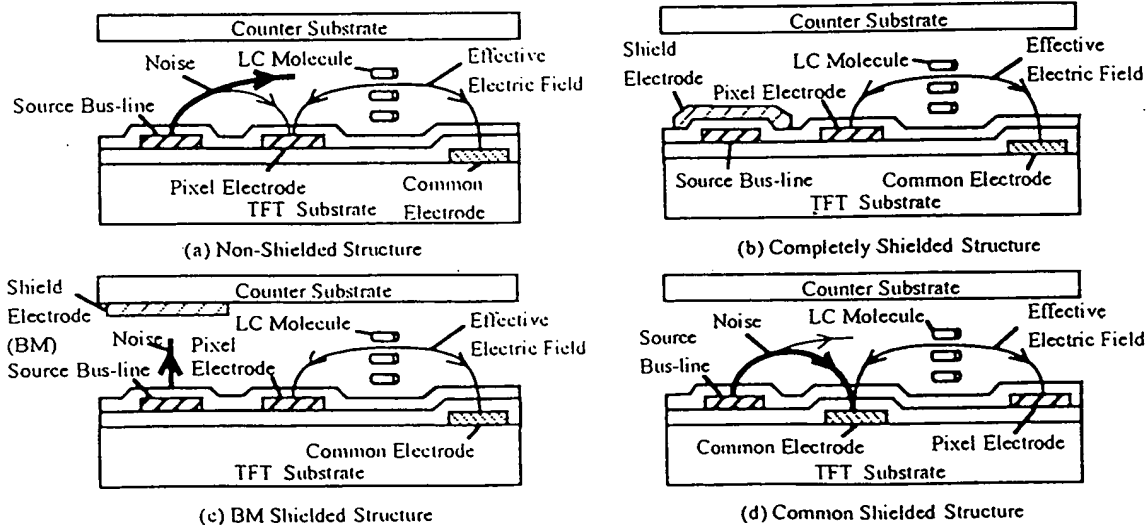


Figure 2. Cross sectional views of layered structure for shielding noise electric field from a source bus-line.

electrode have higher in-plane rotation angles and lower tilt angles than those for the narrow common electrode. This means the LC directors are less affected by the source potential.

Figure 5 shows the relationship between the shielding efficiency  $k$  of the adjacent common electrode and the ratio of  $W_C/W_S$  calculated from the 2-D simulation. Here, we have introduced the concept of shielding efficiency  $k$  which represents the ratio of the average electric field parallel to the substrate to the ideal electric field in the case without the source bus-line. This  $k$  means the ratio of the leakage of the electric force lines from the source bus-line. We expected that shielding was more effective as the width of the common electrode  $W_C$  was increased because the fixed potential of the common electrode would expand farther into the LC layer normal to the substrate plane, and that the shielding was more effective as the width of the source bus-line  $W_S$  was decreased because the potential of the source bus-line would lose intensity normal to the substrate. Looking at figure 5, we see as the ratio of  $W_C/W_S$  increases, the shielding efficiency  $k$  of the adjacent common electrode increases.

Figure 6 shows a schematic diagram of electric fields in a pixel. The electric field in the sub-pixels is represented by the following equations.

$$\begin{aligned} \text{If } i=1 \text{ or } i=m, \\ E_i &= E_{\text{eff}} + (1-k)E_{\text{PS}} \\ \text{If } i \neq 1 \text{ and } i \neq m \\ E_i &= E_{\text{eff}} \end{aligned}$$

where we have assumed the source bus-line potential  $V_S$  is equal to the adjacent source bus-line potential  $V_S'$ .

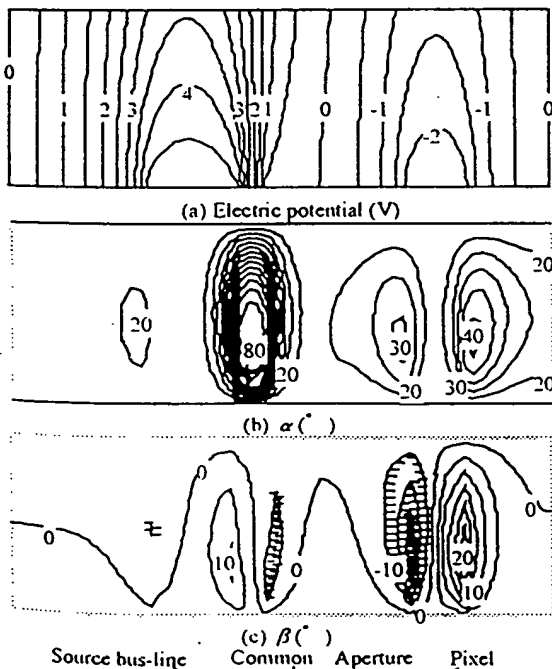


Figure 3. Distributions of (a) electric potential, (b) in-plane rotation angle  $\alpha$  and (c) tilt angle  $\beta$  for  $W_C/W_S=0.6$  (narrow common width)

The parameter  $m$  represents the number of sub-pixels divided by the interdigital electrodes and  $i$  is the sub-pixel number as in figure 6.  $E_i$ ,  $E_{\text{eff}}$  and  $E_{\text{PS}}$  represent the electric field of the sub-pixel  $i$ , the effective electric field applied by the pixel electrode and the common electrode, the electric field between the pixel electrode and the source bus-line, respectively. When a window image pattern which has bar images with width  $T_W$  in the vertical direction has been displayed, the root mean square voltage  $V_{\text{rms}}(T_W)$  between the two electrodes driving the LCs in the aperture areas is expressed by the following equation.

$$V_{\text{rms}}(T_W) = (m/d) \left\{ (1/T) \left( \int \sum E_i^2 dt + \int \sum E_i^2 dt \right) \right\}^{1/2} \quad (2)$$

Here,  $d$  is the distance between the two electrode. Therefore, the crosstalk intensity  $CI$  is represented by the following equation.

$$CI(T) = \Delta B/B = \{ B(V_{\text{rms}}(T_W)) - B(V_{\text{rms}}(T_W=T)) \} / B(V_{\text{rms}}(T_W=T)) \quad (3)$$

Figure 7 compares the simulation results for the shielding efficiency  $k$  and the measured results for test element groups (TEGs) when  $W_C/W_S$  was varied. Good agreement is obtained for the dependence of crosstalk intensity on the window pattern width. Figure 8 shows dependence of the crosstalk intensity  $\Delta B/B$  on the shielding efficiency  $k$  for the white window pattern what a width of  $T_W/T=0.75$ , displayed in the background having 10% relative brightness. When the efficiency  $k$  becomes more than 0.8, the crosstalk intensity drastically decreases.

The above results confirm that most leakage of noise

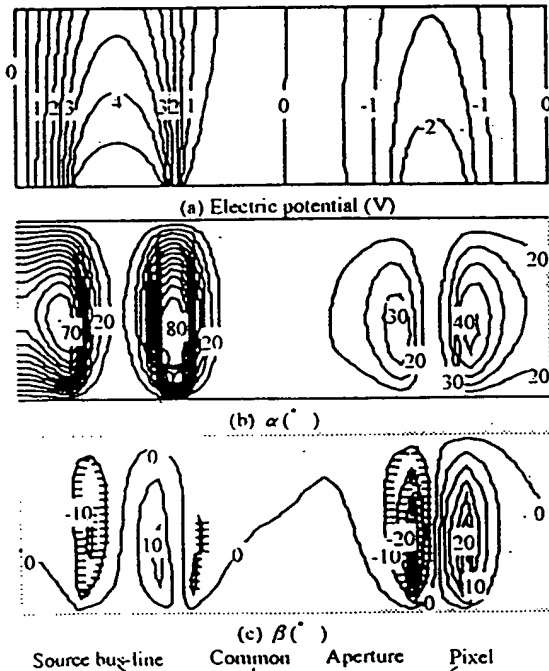


Figure 4. Distributions of (a) electric potential, (b) in-plane rotation angle  $\alpha$  and (c) tilt angle  $\beta$  for  $W_C/W_S=1.5$  (wide common width)

can be shielded by the common shielded structure (figure 1(d)) with the optimized parameter  $W_C/W_S$ .

### Specifications of 13.3 XGA

Using these results, we developed a prototype 13.3 inch diagonal IPS-TFT-LCD with XGA resolution (1024 x 768 x RGB). Table 1 shows its specifications. The crosstalk intensity is less than 5%.

### Summary

Influences of the noise from the source bus-lines to the signal electric field were analyzed to suppress the crosstalk in IPS TFT-LCDs.

From this analysis, we found that crosstalk can be suppressed to a negligible level by using the common shield structure with the optimized parameter ( $W_C/W_S$ ) obtaining the shielding efficiency  $k$  of more than 0.8.

We developed a crosstalk free (crosstalk intensity of less than 5%) IPS TFT-LCD with a large display area (13.3 inch diagonal) and high (XGA) resolution by using the proposed pixel design.

### Acknowledgement

The authors wish to acknowledge Messrs. Z. Odawara, H. Kawakami, K. Kinugawa, Z. Tajima, N. Konishi, and T. Futami of Hitachi, Ltd. for their encouragement and support of this research. We also thank Mr. M. Oh-e for his studies on LC materials for the IPS mode. Finally, we are especially grateful to our co-workers for their assistance in designing and producing the prototype 13.3-in. diagonal IPS TFT-LCD.

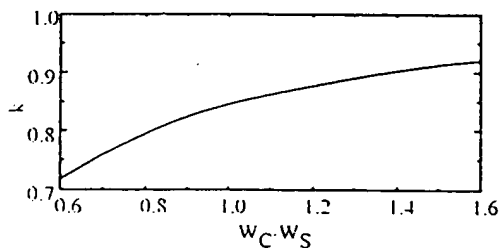


Figure 5. Relationship between shielding efficiency  $k$  of the adjacent common electrode and the electrode width ratio  $W_C/W_S$  (calculation)

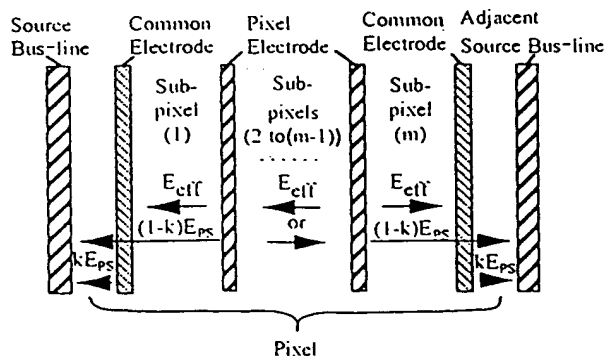


Figure 6. Schematic diagram of electric fields in a pixel

### References

- [1] R. Kiefer, B. Weber, F. Windscheid, G. Baur, Japan Display'92, pp.547-550(1992).
- [2] G. Baur, Abstract of 22. Freiburger Arbeitstagung Flüssigkristalle(1993).
- [3] G. Baur, Abstract of 23. Freiburger Arbeitstagung Flüssigkristalle(1994).
- [4] G. Baur, M. Kamm, H. Klausmann, B. Weber, B. Wieber and F. Windscheid, 15th International Liquid Crystal Conference, Abstract No. K-P15(1994).
- [5] M. Oh-e, M. Ohta, K. Kondo and S. Oh-hara, 15th International Liquid Crystal Conference, Abstract No. K-P17(1994).
- [6] M. Oh-e, M. Ohta, S. Aratani and K. Kondo, Asia Display'95, pp.577-580(1995).
- [7] M. Oh-e and K. Kondo, Appl. Phys. Lett., 67, 3895(1995).
- [8] M. Oh-e, M. Ohta, and K. Kondo, Abstract of 25. Freiburger Arbeitstagung Flüssigkristalle(1996).
- [9] M. Ohta, M. Oh-e and K. Kondo, Asia Display'95, pp.707-710(1995).
- [10] M. Ohta, K. Kondo and M. Oh-e, IEICE TRANS. ELECTRON., VOL. E79-C, NO.8 AUGUST(1996).
- [11] Dickmann, S. et al., SID'93 Digest p.638(1993).
- [12] Dickmann, S. et al., Freiburger Arbeitstagung Flüssigkristalle(1994).

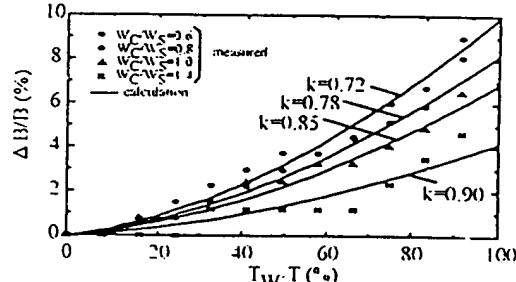


Figure 7. Dependence of crosstalk intensity  $\Delta B/B$  on window pattern width  $T_W/T$

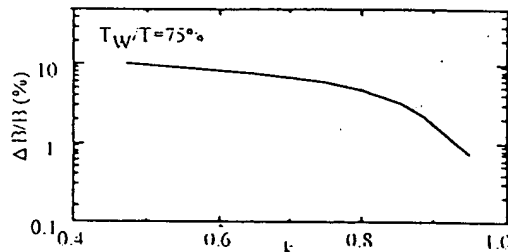


Figure 8. Dependence of crosstalk intensity  $\Delta B/B$  on shielding efficiency  $k$

Table 1. Specifications of the prototype 13.3-in. diagonal IPS TFT-LCDs

Display Area	13.3 inch diagonal
Number of Pixels	1024(H) × 768(V) × RGB
Dot Size	0.088mm(H) × 0.264mm(V)
Number of Colors	262,144
Viewing Angle	H: ±70° V: ±70°
Contrast Ratio	>100
Driving Voltage of Signal Driver	5V
Response Time ( $\tau_f + \tau_r$ )	70ms(35ms+35ms)
Crosstalk Intensity	H: <5% V: <5%

\*1: Maximum viewing angles where contrast ratio >10 and non gray scale reversal (8 gray scales)  
\*2:  $\Delta B/B$  where ratio of window pattern width  $T_W/T=0.75$  and relative brightness of back-ground area = 10%

*Here Dr. Fleck*  
BEST AVAILABLE COPY PS-Papers.

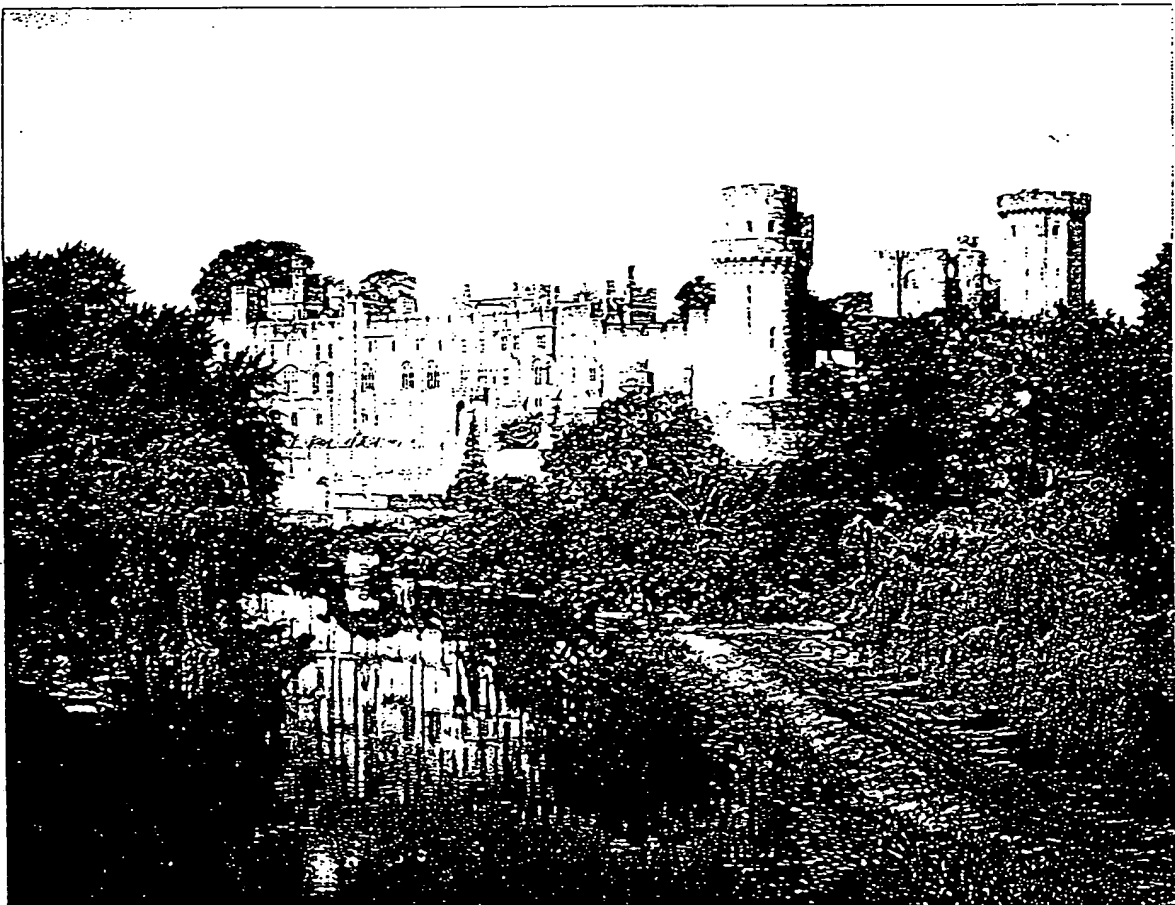
*MFA Galleries*  
*27.10.96*

**SID**  
SOCIETY FOR INFORMATION DISPLAY

**EURODISPLAY**

## Proceedings of the 16th International Display Research Conference

*Warwick Castle, the finest mediæval Castle in England*



Metropole Hotel & Conference Centre,

NEC, Birmingham, England

October 1 – October 3, 1996